Proceedings of the 3rd ITB Graduate School Conference ISSN: 2963-718X
Enhancing Creativity in Research Through Developing Innovative Capabilities
December 21, 2022

Identifying Collapse of Topography Using Temporal Pansharpened Optical Images at Active Volcano: Case Study of Mt. Semeru Eruptions in 2021

Vismaia Isanjarini & Asep Saepuloh*

Geological Engineering Study Program, Faculty of Earth Sciences and Technology, Bandung Institute of Technology, Indonesia.
*Email: saepuloh@itb.ac.id

Abstract. Mt. Semeru is one of active volcanoes in Java. The eruption material released by Mt. Semeru is in the form of unconsolidated volcanic material. The nature of the material is very easy to erode and collapse. The eruption that occurred in 2021 caused disruption to critical infrastructure, ranging from power cuts and the collapse of the main bridge. The collapsed topography was assumed to have caused the massive eruption in 2021 but was not detected by monitoring equipment at the time. To observe the phenomenon, the Landsat-8 and PlanetScope images were used. The Gram-Schmidt transformation was conducted to increase the spatial resolution of Landsat-8 image 30 m to Planetscope image 3 m. This method was applied to the images before and after the 2021 eruption for determining the possibility of a collapse topography. According to the visual pansharpened images, we could identify the collapse topography in the eastern sector following the eruption. The collapse sector formed landslide with quite deep incision about 650 m. The collapsed materials accumulated in the SE-flank of Kobokan drainage and sent down the pyroclastic flows about 700 m to the valley.

Keywords: *Collapse, Gram-Schmidt, Pan-Sharpening, Mt. Semeru.*

1. Introduction

Mt. Semeru is in Lumajang and Malang Regencies, East Java. Mt. Semeru is one of the most active volcanoes in Java. Hundreds of eruptive events in Mt Semeru occurred during the 19th and 20th centuries, it has been persistent since 1967. An eruption and dome collapse occurred near the summit on 4 December 2021, which produced a notable ash plume and pyroclastic flows, the latter of which generated major lahars [1]. Eruption material released by Mt. Semeru is in the form of unconsolidated volcanic material. The nature of the material is very easy to erode and collapse. As a result, several communities were partially buried, causing fatalities, disruption to critical infrastructure, ranging from power cuts and the collapse of the main bridge. The collapsed topography was assumed to have caused the massive eruption in 2021 but was not detected by monitoring equipment at the time. So, the aim of this research is to observe the topographical collapse that occurs because of the eruption.

Remote sensing techniques provide the opportunity to study active and dangerous volcanoes, allowing us to safely observe topography details over a large area. This is particularly true for Mt Semeru, as one of active volcano in Indonesia. Standard remote sensing techniques using high-spatial resolution images from PlanetScope offer a fruitful means with which to characterize the volcano's topography and to recognize the extent and effects of the eruptive processes.

To observe topography collapse, both Landsat-8 and PlanetScope were used. Gram schmidt transformation was conducted to pansharp Landsat-8 and PlanetScope data. In this method the statistical values of the high-resolution bands are adjusted to the values of the first transformation bands to produce a new set of transformation bands resulting in sharpened multispectral data. Gram-Schmidt has become one of the most popular algorithms for pan-sharpen multispectral images [2]. This method outperforms most other pan-sharpen methods in maximizing image sharpness, minimizing color distortion, and the most optimal method for collapse detection [5]. Gram-Schmidt is generally more accurate because it uses the spectral response function of a given sensor to approximate the appearance of the panchromatic data. This method was used on the images before and after the 2021 eruption to determine the possibility of collapse.

The Semeru-Tengger volcanic massif with an area of about 900 km^2 comprises a cluster of calderas and strato-cones aligned from north to south over 25 km, including: the Bromo-Tengger, Jambangan and Ajek-Ajek calderas; the Mt. Kepolo lava cone; and the composite cone of Mt. Mahameru-Semeru **(Figure 1)**. The recent composite cone of about 60 km^3 [9] has not been dated, but maybe Late Pleistocene to Holocene in age. The twofold edifice (Mahameru and Young Semeru) has been superimposed on, and but tressed to the N, by the Jambangan complex. To the S and SE Semeru overlies weathered volcaniclastic sediments and lava flows of the Oligocene–Miocene ‘Tuff and Old Andesite formation [8]. The equatorial monsoon climate produces as much as 2000 to 3700 mm per year on the E and SE flanks of Semeru while 200 mm of rain can fall in 24 h every 5 years on average [6].

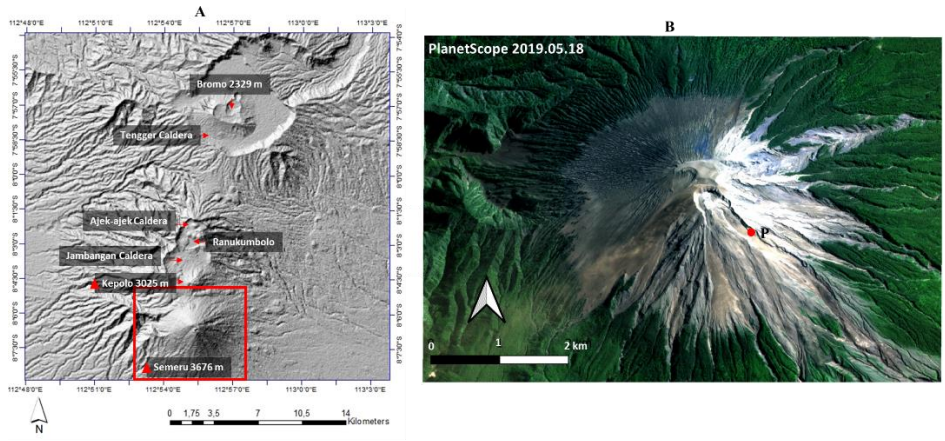

Figure 1 Digital Elevation Model (DEM) Mt. Semeru and its surrounding (A) and the natural color composite of Planetscope image with acquisition time May 18th, 2019, shows the morphology of Mt. Semeru (B).

2. Data used and selection

In this study we have selected Landsat-8 and PlanetScope. Landsat 8 imagery has 11 bands where there are different spatial resolution values for each band. In bands 1,2,3,4,5,6,7,9 it has a spatial resolution of 30 meters. Bands 10 and 11 have a spatial resolution of 100 meters. And band 8 has a spatial resolution of 15 meters. With the Pan-Sharpening technique, it can increase the spatial resolution of the composite bands by adding band 4,3,2 (natural color) from 30 m to 3m. Previously done pre-processing radiometric calibration and atmospheric correction. But for the images during the eruption and after the eruption which is landsat-8 collection 2 level 2 no pre-processing is required, because this data is already atmospherically corrected. To validate it, a spectral check was carried out (**Figure 2**). 10 scenes have been used under acquisition mode from January 28th, 2019 to August 22th, 2022 (**Table 2**).

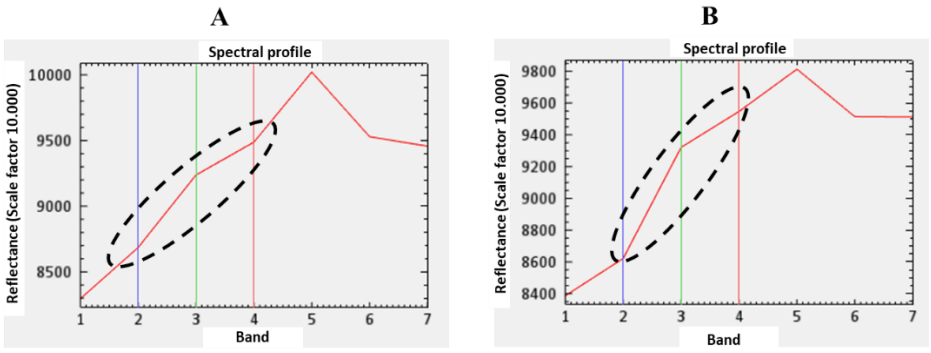

Figure 2 Spectral bands on the image during the eruption and after the eruption at SE trending scar on February 3, 2022 (A) and August 22, 2022 (B).

The following is a spectral validation where the blue band is lower than the red band and green band. In theory the blue band has a lower spectral value compared to the green band because it has a shorter wavelength. This indicates that this image has been corrected.

Planetscope images have used because of high resolution image about 3 m capable to observe topography. The data is available freely under proposed academic term and condition. The PlanetScope provides the image data for analytic basic, visual ortho, analytic ortho, visual ortho tile, and analytic ortho tile scenes. Orto tile image have been used because it provided 4-band multispectral image in blue (band 1), green (band 2), red (band 3), near-infrared (band 4). All of its bands have a resolution of 3 m. The detail specifications of PlanetScope wavebands are listed in **Table 1**.

Table 1 Bands description of the selected 4-band multispectral of PlanetScope images [3].

Number	Name	Description	Wavelength (nm)
1	B1	Blue	465-515
2	B2	Green	547-585
3	B3	Red	650-680
4	B4	Near Infrared	845-885

The 4-band multispectral of PlanetScope images has been processed at level 3B which is corrected geometrically and atmospherically. Comparisons were made among bands 1, 2, 3 and 4 for pansharpening method with landsat 8 (**Figure 2**). Based on this comparison, panhsarpening with band 4 (NIR) produces a clearer collapse topography and minimal distortion, because the wavelength of the Near

Infrared (NIR) is sensitive to collapse and on the histogram it can be seen that band 4 is normally distributed. So, in this pansharpening method we use the combination of landsat-8 multispectral data with planetary NIR band.

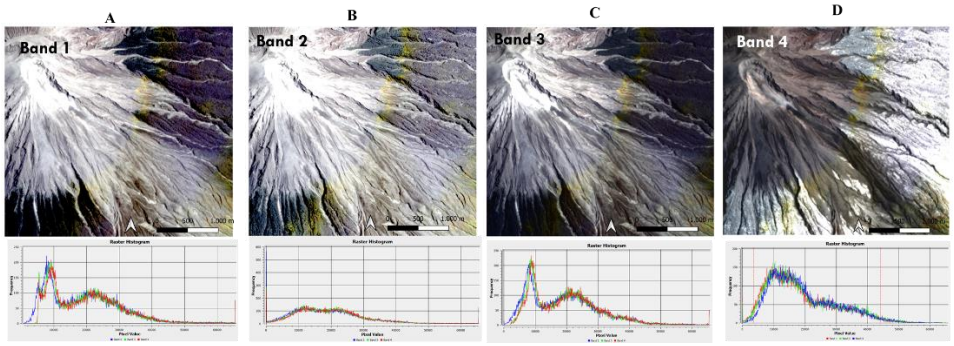

Figure 3 Visual of pansharpened images using PlanestScope image bands-1 (A), band-2 (B), band-3 (C), and band-4 (D) and their histograms.

The following is the available data with a minimum cloud (<10%) that can be used in this method **(Table 2)**. The years before (2019, 2020, 2021) and after (2022) the eruption is used to see the impact caused by the eruption. This pansharpening method is used when there are only Landsat images so that sharpening is needed, thus it is as if you have many planetScope images.

Table 2 The available data with a minimum cloud (<10%).

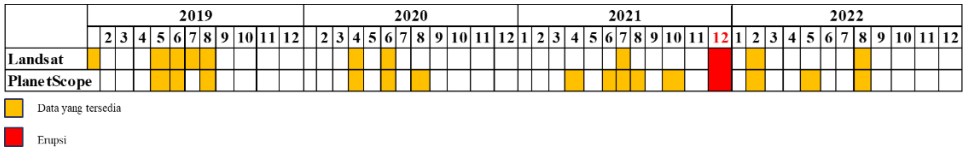

Table 3 The selected PlanetScope and Landsat-8 image used in this study with cloud cover less than 10% for each frame.

Image	Acquisition Date	Cloud Coverage	Event
PlanetScope	May 18th, 2019	3%	Before eruption
	June, 18th 2019	1%	
	August, 16th 2019	5%	
	April, 10th 2020	4%	
	April, 21st 2020	3%	
	June, 13th 2020	7%	
	August, 22nd 2020	3%	

	April, 19th 2021	1%	
	June 30th, 2021	8%	
	July, 2nd 2021	4%	
	August 26th, 2021	6%	
	Oktober, 17th 2021	0%	
	Desember, 13th 2021	3%	After eruption
	Febuary, 3rd 2022	3%	
	May 15th, 2022	9%	
	August 1st, 2022	2%	
Landsat-8	Januari 28th, 2019	2%	Before eruption
	May 18th, 2019	3%	
	Juni, 11st 2019	2%	
	Juni, 18th 2019	4%	
	July, 13th 2019	1%	
	August, 16th 2019	3%	
	April, 10th 2020	6%	
	June 13th, 2020	7%	
	July 2nd , 2021	2%	
	Febuari, 3rd, 2022	5%	After eruption
	August 22th, 2022	3%	

3. Method

The combination of panchromatic and multispectral images is known as pansharpening. Pansharpening is generally a method for combining high-resolution spatial values from panchromatic images with low-resolution multispectral images. In general, two or more images are integrated into one image by maintaining the important features. The resulting quality of the stitched images is related to many factors such as spatial, spectral, radiometric accuracy and distortion. Therefore, different pansharpening methods have been developed with different objectives.

Since its publication in 1998, the Gram-Schmidt pan-sharpen method has become one of the most popular algorithms for pan-sharpen multispectral images [2]. This method outperforms most other pan-sharpen methods in maximizing image sharpness, minimizing color distortion, and is the most optimal method for landslide detection [5]. Gram-Schmidt is generally more accurate because it uses the spectral response function of a given sensor to approximate the appearance of the panchromatic data.

Orthogonalization is the process of discovering two vectors that are at 90 degrees to each other. When two vectors are orthogonalized, they will become

orthonormal to each other. The gram-scmidt process is the process of converting a set of vectors into an orthonormal basis. The projection operator can be defined as followed:

$$Proj_u\ (v) = \langle \frac{u,v}{v,v} \rangle\ u \quad (1)$$

u and *v* are two vectors. <*u*, *v*> is the inner product of the two vectors, showing the component of *u* in the direction of *v*. When <*u*, *v*> = 0, the two vectors are orthogonal (at right angles with each other). This operation causes a projection transformation of the vector *v* in the line on which *u* is situated.

The Gram-Schmidt process uses this operator to compute two sequences, $u_1 \ldots u_i$ and $n_1 \ldots n_i$:

$$U_1 = v_1\ , n_1 = \frac{U_1}{||U_1||} \quad (2)$$

$$U_2 = v_2 - Proj_{u1}\ (v_2\ ), n_2 = \frac{U_2}{||U_2||} \quad (3)$$

$$U_3 = v_3 - Proj_{u1}\ (v_2\ ) - Proj_{u1}(v_3\ ), n_3 = \frac{U_3}{||U_3||} \quad (4)$$

$$U_k = v_3 - (x+a)^n = \sum_{i=1}^{k-1} Proj_{u1}\ \ (v_k\ ), n_k = \frac{U_k}{||U_k||} \quad (5)$$

The sequence $u_1 \ldots u_i$ is the set of orthogonal vectors. To calculate u_i, this process essentially transforms vi using the projection transformation onto the linear subspace created by $u_1 \ldots u_i$. u_i is therefore the difference between vi and this subspace. Calculating the sequence $u_1 \ldots u_i$ is Gram-Schmidt orthogonalization, giving us the required set of orthogonal vectors while calculating the vector set $n_1 \ldots n_i$ is Gram-Schmidt orthonormalization.

The first step in pansharpening using the Gram-Schmidt method is to create a high-resolution NIR band that matches the resolution of the multispectral bands. Next, the multispectral bands are decorrelated. Each one is treated as one multi-dimensional vector, with each pixel being one dimension. The greater the number of pixels, the greater the number of dimensions. This decorrelation is done using the Gram-Schmidt process. The high-resolution NIR band which we computed is taken as the first vector, u1. The multispectral bands are correlated and orthogonalized to this band. Next, the low-resolution band is replaced by the high-resolution one. The multi-spectral bands transform in the same way as the high-resolution NIR band. This produces high-resolution versions of themself.

The following is the result of pansharpening gram schmidt which is a combination of Landsat images with a resolution of 30 m multispectral band with

NIR planetscope images with a resolution of 3 m so that the resolution becomes 3 m (**Figure 3**). In the initial image (multispectral), object observed is not very clear, whereas in the pansharpening image can be seen much more detail. The panhsarpening image has information details such as NIR. Whereas for the color elements follow the multispectral. But, in some appearances, does not match the natural color, this is due a difference in the acquisition time of the two types data.

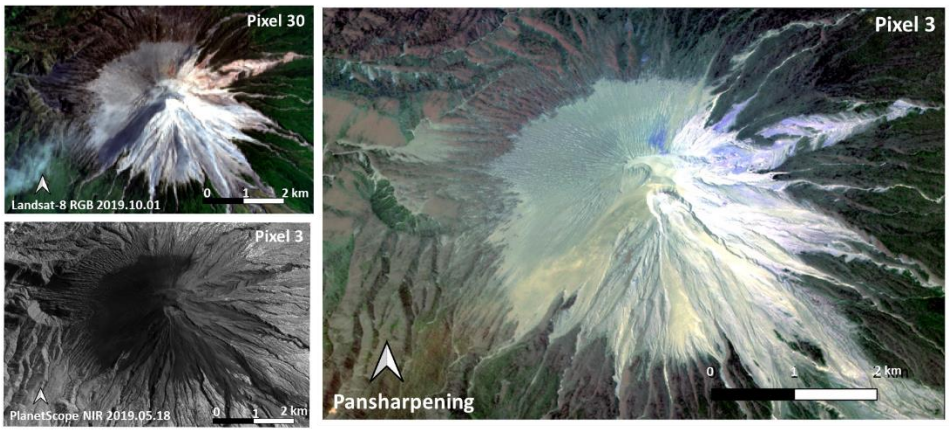

Figure 4 Pansharpening method scheme

4. Result and Discussion

The Gram-Schmidt transformation was conducted to pan-sharpening landsat-8 and planetscope image. This method was used on the images before (2019, 2020, 2021) and after eruption (2022) to determine the possibility of a collapse topography. Pansharpening results were evaluated using a qualitative approach which involves a visual comparison of the colors among the multispectral image, the NIR image and the pansharpening image [10]. To observe the visual appearance of the results pan-sharpening, this research takes a few samples for differences in visual appearance between landsat-8, planetscope and pansharpening images using the GramSchimdt method. The results of observations are as follows:

4.1 Before Eruption

There are 16 scenes taken from 2019-2021 to observe the appearance before the eruption. Based on the results of pansharpening before the eruption, it can be seen there is no volcanic activity, and there is no collapse detected. The upper northeastern flank of the summit cone appears more weathered, comprising

reddish brown, and unconsolidated deposits. For this reason, an image observation was carried out during and after the eruption to see if there was a collapse in Semeru on December 2021.

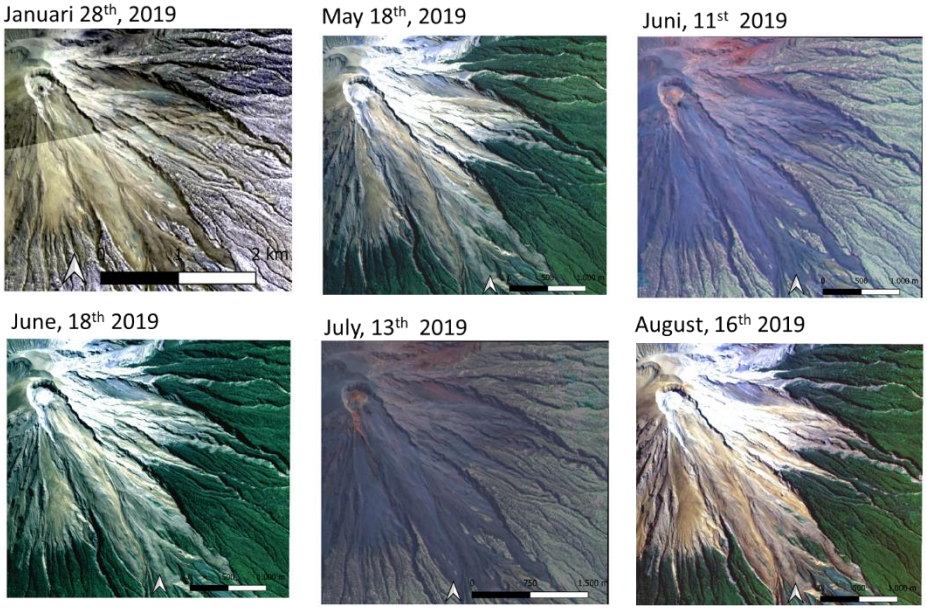

Figure 5 Observation through PlanetScope image in 2020 composite band 4 3 2 to see the appearance before collapse topography

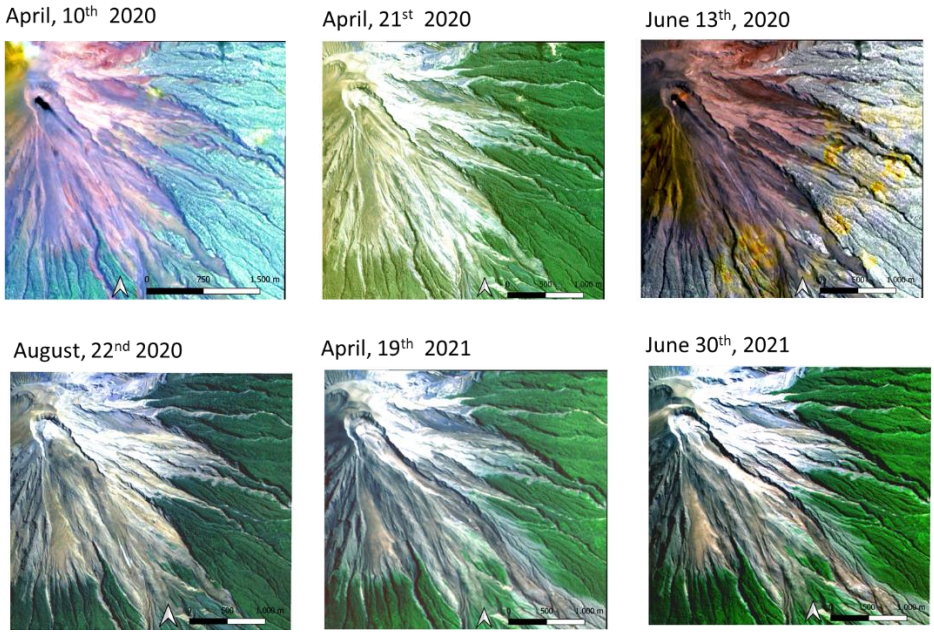

Figure 6 Observation through PlanetScope image in 2020 composite band 4 3 2 to see the appearance before collapse topography

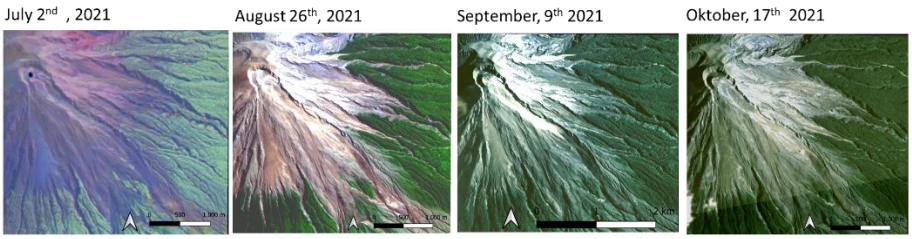

Figure 7 Observation through PlanetScope image in 2021 composite band 4 3 2 to see the appearance before collapse topography

4.2 After Eruption

In the analysis after the eruption used landsat data on August 22rd 2022 while the planet on June 29th 2022 because at that time it was very clear (not covered by clouds) so observations were easier. Collapse suspected like a pressure release valve that allowed magma to spew forth rapidly, escaping the volcano before crystals had had a chance to grow. Based on the results of pansharpening after the eruption, it can be seen collapses trace in the eastern part of Mt. Semeru.

Collapse dome also happened in Semeru's Jonggring Seloko Crater and SE-flank flow. It is also proven by almost all of the houses in the Curah Kobokan area had been destroyed, mainly by pyroclastic flows, though some residents reported roof collapses from ashfall [4]. Lava flows have filled the Kobokan head valley from the Jonggring-Seloko crater. As a result, the valley channel will become an area of aggradation produced by lava front collapses, which will be remobilized by rain-triggered lahars during the next rainy seasons.

Figure 8 Observation through PlanetScope image in 2022 composite band 4 3 2 to see the appearance after collapse topography

4.3 Pansharpening Evaluation

Pan-sharpening techniques can result in spectral distortions when pan sharpening satellite images as a result of the nature of the NIR band. The planetscope NIR band for example is not sensitive to blue light. As a result, the spectral characteristics of the raw NIR color image may not exactly match those of the corresponding low-resolution RGB image, resulting in altered color tones (**Figure 9**). This has resulted in the development of many algorithms that attempt to reduce this spectral distortion and to produce visually pleasing images. The following is an image before and after the eruption resulting from pansharpening which shows a collapse in the eastern part of Mount Semeru (**Figure 9**). This collapse material is transported up to 650m to the SE-flank Kobokan drainage. The results of these visual observations were then validated with existing secondary data which indicated that a collapse would occur in 2021. Based on PVMBG 2021, the seismic network recorded avalanche signals. Avalanches of incandescent material from the summit dome and SE-flank lava flows descended 500-800 m. Evidence of this collapse can be seen in the pansharpening images where there is an accumulation of collapsed material. Then these results were analyzed quantitatively

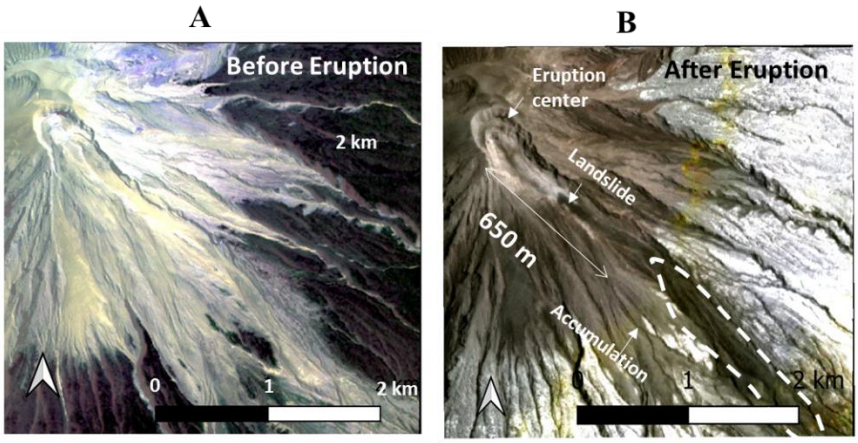

Figure 9 Pansharpening before (A) and after eruption (B)

Before pansharpening the pixel value is 30 m (x=125, y=114), then after pansharpening the pixel value changes to 3 m (x=1239, y=1134). Based on data, it was found that there was a change in the number of columns and rows in the image as well as the value of the digital image which indicated a change in image quality due to pansharpening. For this reason, image quality measurements are taken in the form of min, max, mean, and standard deviation (**Table 3 and 4**).

Table 4 Pansharpening quality measurement before eruption

Parameter	**Multispectral Landsat-8 (May 18th, 2019)**		
	Band 4 (red)	**Band 3 (green)**	**Band 2 (blue)**
Min	44	117	283
Max	4500	4076	3797
Mean	1157.8613905857	1183.5982977003	1078.7027263744
Standard deviation	682.58750780715	542.74476831045	552.91122531322
Parameter	**Planetcope (October 1st, 2019)**		
	Band 4 (NIR)		
Min	287		
Max	5099		
Mean	1710.718360039		
Standard deviation	802.61895315428		

Parameter	Pansharpening		
	Band 1 (red)	**Band 2 (green)**	**Band 3 (blue)**
Min	0	0	0
Max	981	938	1286
Mean	265.56345064744	408.22645916561	410.18563867751
Standard deviation	158.39913626069	141.96910617941	237.60461611649

Table 5 Pansharpening quality measurement after eruption

Parameter	Multispectral Landsat-8 (June 29th, 2022)		
	Band 4 (red)	**Band 3 (green)**	**Band 2 (blue)**
Min	4665	4922	373
Max	41279	40551	41996
Mean	14336.107146065	14097.481876572	13557.467984278
Standard deviation	9379.4475299996	9191.0299996829	9583.7508428908
Parameter	**Planetcope (August 22th, 2022)**		
	Band 4 (NIR)		
Min	531		
Max	5545		
Mean	1364.1652752376		
Standard deviation	653.88059427796		
Parameter	**Pansharpening**		
	Band red	**Band green**	**Band blue**
Min	0	0	0
Max	65535	65535	65535
Mean	13896.135166337	13659.617535142	13150.007287068
Standard deviation	9153.6296325029	9070.5203865447	9319.9147597041

Based on this table:

1. Min and max between the previous images are greater than the sharpened images, but the number of pixels in the pansharpening image is greater.

2. The mean value of the image before it is sharpened is much larger than the image after it is sharpened. This is because the density of the sharpened image increases and automatically the value of M (row) and N (column) as the divider of the number of pixel values is greater than the image before sharpening. So that the image analysis of the mean value shows that the sharpened image has a smaller mean because it has more row and column sizes. Based on the results of the Mean value, the image before sharpening has a larger value compared to the image that has been sharpened as well as the Standard Deviation value, so it can be concluded that after sharpening the pixel density increases and makes the image clearer.
3. Standard deviation (SD) before it is sharpened has a greater value than the image after it is sharpened. Standard Deviation is a reflection of the average deviation of the data from the mean. The Standard Deviation can describe how far the data varies. If the SD value is much greater than the mean value, the mean value is a bad representation of the entire data. Based on these data, the standard deviation value before pansharpening can be used as a representation of the entire data.

5. Conclusion

The results of the processing are in the form of suspected collapse topography which are characterized by the morphology in the eastern sector which appears in pan-sharpening images after the eruption. In the eastern part of Mount Semeru, it was seen that there was a landslide which was quite deep. Material collapsed from the unstable distal end of a 650m in the SE-flank Kobokan drainage, sending a pyroclastic flow 700 m down the valley. The results of this pansharpening were evaluated using quantitative analysis (min, max, mean, and standar deviation), which shows that pansharpening image can be used as a representation of the entire data.

Reference

[1] Bennis, K.L., and Andrews, B., eds. *Report on Semeru (Indonesia): Semeru (Indonesia) Pyroclastic flows, gas-and-ash emissions, and crater incandescence during January-June 2022.* Bulletin of the Global Volcanism Network, **47**:7. Smithsonian Institution.2022.

[2] Laben CA, Bernard V., Brower W. *Process for Enhancing the Spatial Resolution of Multispectral Imagery Using Pan-Sharpening*, US Patent. 2000.

[3] Planet. *Planet Imagery Product Spesification PlanetScope and RapidEye*. 2016

[4] Pusat Vulkanologi dan Mitigasi Bencana Geologi (PVMBG, also known as CVGHM). *Semeru Eruption on Desember 2021*. 2021.

[5] Santurri, L., Carlà, R., Fiorucci, F., Aiazzi, B., Baronti, S., Cardinali, M., dan Mondini, A. C. *Assessment of very high resolution satellite data fusion techniques for landslide recognition*, ISPRS Technical Commission VII Symposium, 100 Years ISPRS {\textendash} Advancing Remote Sensing Science, **38**, 1–6. 2010.

[6] Siswowidjoyo, S., Sudarsono, U., & Wirakusumah, A.D. *The threat of hazards in the Semeru volcano region in East Java, Indonesia*. Journal of Asian Earth Sciences, **15**, 185- 194.1997.

[7] Solikhin, A. *Geology , tectonics and post-2001 eruptive activity interpreted from high-spatial resolution satellite imagery : the case study of Merapi and Seremu volcanoes , Indonesia*, Doctoral School of Funfamental Sciences Universite Blaise Pascal.2015.

[8] Sutawijaya, I.S., Wahyudin, D., dan Kusdinar, E. *Peta geologi Gunung Api Semeru, Jawa Timur*, Direktorat Vulkanologi, Bandung.1996

[9] Thouret, J.-C., Lavigne, F., Suwa, H., Sukatja, B., Surono. *Volcanic hazard at MountSemeru, East Java (Indonesia), with emphasis on lahars*. Bulletin of Volcanology. **70**, 221–244. 2007

[10] Zhang, Yun. *Methods for Image Fusion Quality Assessment – A Review, Comparison and Analysis*. The International Archives of the Photogrammetry. Remote Sensing and Spatial Information Sciences. **38**. 2008.